



Dimensional Crossover in the Nb/Al₂O₃ Josephson-Coupled Multilayers

Manabu IKEBE, Yoshihisa OBI¹, Hiroyuki FUJISHIRO
and Hiroyasu FUJIMORI¹

*Department of Materials Science and Technology, Faculty of Engineering,
Iwate University, Morioka 020*

¹*Institute for Materials Research, Tohoku University, Sendai 980*

(Received May 6, 1993)

The dimensional crossover from anisotropic three-dimensional to two-dimensional behavior in the temperature dependence of the parallel critical field has been studied for Nb/Al₂O₃ superconductive multilayers as a function of the structural modulation wavelength λ . The thicknesses of the superconductive Nb sublayer (d_{Nb}) and the Al₂O₃ tunneling barrier sublayer ($d_{\text{Al}_2\text{O}_3}$) were varied up to 100 Å. In accord with the calculation due to Deutscher and Entin-Wohlman, the crossover occurs in the vicinity of T^* , where the perpendicular coherence length $\xi_{\perp}(T)$ satisfies the relation, $1.4\xi_{\perp}(T^*)=\lambda$, irrespective of the ratio λ/d_{Nb} .

[superconductivity, Nb/Al₂O₃ multilayer, superlattice, upper critical field,]
dimensional crossover

§1. Introduction

The superconductors with layered structure show typical anisotropic and/or two-dimensional (2D) properties. Among those characteristic properties, the dimensional crossover in the parallel critical field ($H_{c2\parallel}$) is the most conspicuous and has been the subject of several investigations.¹⁻⁵⁾ This phenomenon is qualitatively understood in the following way. Near T_c , where the interlayer coherence length $\xi_{\perp}(T)$ is longer than the structural modulation wavelength λ , $H_{c2\parallel}(T)$ is proportional to $(T_c - T)$ in accord with the three-dimensional (3D) Ginzburg-Landau (GL) theory.⁶⁾ Below a certain temperature T^* , at which $\xi_{\perp}(T)$ becomes nearly equal to λ , $H_{c2\parallel}$ behavior changes to that of a thin film and $H_{c2\parallel}(T)$ diverges if we neglect the layer thickness and Pauli paramagnetic effect.⁷⁾ Such behavior of H_{c2} is designated as quasi-2D superconductivity. The dimensional crossover was initially observed in naturally occurring compounds, *e.g.*, intercalated transition metal dichalcogenides.⁸⁾ With the recent development of the deposition technique, the crossover has also been observed for many types of artificial multilayers, *e.g.*, Nb/Ge,¹⁾ Nb/Cu,²⁾ Nb/Ti,⁹⁾

V/Ag¹⁰⁾ etc.

The artificial multilayer superconductors may be divided into two main types according to the nature of the interlayer coupling. One type is the superconductor/metal multilayer in which the proximity effect is responsible for the coupling.¹¹⁻¹⁴⁾ The other type is the superconductor/insulator multilayer in which Josephson tunneling provides the coupling.^{15,16)} Experimentally, the dimensional crossover in the proximity-effect-coupled multilayers has been rather thoroughly investigated and detailed theoretical treatment has been given by Takahashi and Tachiki.^{14,17,18)} While the theoretical study on the layered superconductor was originated by Lawrence and Doniach¹⁵⁾ for the Josephson-coupled model, the experimental study on Josephson-coupled multilayers is scarce except for the pioneering work due to Ruggiero *et al.*¹⁾ on Nb/Ge. In this paper, we examine the dimensional crossover of the Nb/Al₂O₃ multilayers. Because Al₂O₃ is a genuine insulator and Ge is a semiconductor, Nb/Al₂O₃ is expected to be a more ideal Josephson-coupled system than Nb/Ge. The synthesis and characterization of the Nb/Al₂O₃ multilayers have been described previously.^{19,20)} The critical field measurement has

been made resistively by use of a standard four-lead method.

§2. Theoretical Background

Layered superconductors can be considered as bulk or three-dimensional (3D) as long as the interlayer coherence length $\xi_{\perp}(T)$ is larger than the structural modulation wavelength λ by far. In this case, the upper critical fields parallel and perpendicular to the layer are given on the basis of the anisotropic GL theory by

$$H_{c2\parallel}(T) = \frac{\phi_0}{2\pi\xi_{\parallel}(T)\xi_{\perp}(T)} \quad (1)$$

$$H_{c2\perp}(T) = \frac{\phi_0}{2\pi\xi_{\parallel}(T)^2} \quad (2)$$

where $\xi_{\parallel}(T)$ is the intralayer coherence length and ϕ_0 is the flux quantum. In the anisotropic GL theory, effective GL masses parallel and perpendicular to the layer are defined by the following relation,

$$(m_{\perp}/m_{\parallel})^{1/2} = \frac{dH_{c2\parallel}/dT}{dH_{c2\perp}/dT} \Big|_{T=T_c}, \quad (3)$$

In the Josephson-coupled model due to Lawrence and Doniach (LD),¹⁵⁾ layered superconductors are pictured as a stacked array of superconducting layers (with negligible thickness) weakly coupled through Josephson tunneling between adjacent layers. For field orientations except nearly parallel to the layer, the $H_{c2}(T)$ curves of LD theory are essentially the same as those predicted by the anisotropic GL theory. For $H_{c2\parallel}(T)$, however, the LD theory predicted quite anomalous behavior,

$$H_{c2\parallel}(T) \propto 1/[1 - 2\lambda^2/\xi_{\perp}^2(T)]^{1/2}. \quad (4)$$

Thus $H_{c2\parallel}$ diverges at a temperature T^* given by a relation

$$\xi_{\perp}(T^*) = \lambda/\sqrt{2}. \quad (5)$$

Klemm, Luther and Beasley¹⁶⁾ (KLB) extended the LD model and developed a microscopic theory. According to KLB, a characteristic parameter γ is defined by the following equation

$$\gamma = J^2\tau/T_c = \frac{4}{\pi} \left| \frac{\xi_{\perp}(0)}{\lambda/2} \right|^2, \quad (6)$$

where J is the tunneling energy and τ is the total electron scattering time. The parameter γ characterizes the degree of superconductive two-dimensionality, the smaller γ values indicating the stronger 2D characteristics. For $\gamma < 1.76$, the KLB theory reproduced the $H_{c2\parallel}$ divergence and the Pauli paramagnetic limiting was taken account of to remove the unphysical divergence. In case that the interlayer Josephson-coupling is not so weak, the LD-KLB theory also reduces to the anisotropic GL theory. Then, in terms of the KLB theory, the mass ratio in eq. (3) is given by

$$(m_{\perp}/m_{\parallel}) = 2D/J^2\tau\lambda^2, \quad (7)$$

where D is the electron diffusion constant.

The KLB theory, however, neglected the superconducting layer thickness d_s . If we take into account the effect of finite d_s , the $H_{c2\parallel}$ divergence of the Josephson-coupled array should be limited by the H_{\parallel} value of a single layer which is given by

$$H_{\parallel} = \frac{\sqrt{12}\phi_0}{2\pi\xi_{\parallel}d_s}. \quad (8)$$

Based on the KLB theory, Deutscher and Entin-Wohlman (DE)²¹⁾ calculated $H_{c2\parallel}(T)$ of Josephson-coupled layer superconductors keeping d_s finite and found that the crossover manifests itself as an upturn in the $H_{c2\parallel}(T)$ curve. DE pointed out that the condition for the dimensional crossover is given by

$$\lambda/\xi(T^*) \approx 1.4 \quad (9)$$

independent of the λ/d_s value. By comparing eq. (9) with eq. (5) we notice that eq. (8) retains its validity to the limit of $d_s=0$, the limit treated by the LD-KLB theory. Thus we can also expect that the γ parameter defined by eq. (6) may be meaningful also in the finite d_s situation to characterize the superconductive dimensionality. In the following section, the prediction of eq. (9) due to Deutscher and Entin-Wohlman is examined for the Nb/Al₂O₃ artificial multilayers.

§3. Results and Discussion

The upper critical fields of Nb/Al₂O₃ multilayers with Nb and Al₂O₃ layer thicknesses (d_{Nb} and $d_{\text{Al}_2\text{O}_3}$) ranging from 5 Å to 100 Å have been measured under the magnetic field

up to 90 kOe. For the present Nb/Al₂O₃ superlattice, d Nb corresponds to d_s in the previous section and λ is given by the sum of d Nb and d Al₂O₃,

$$\lambda = d\text{Nb} + d\text{Al}_2\text{O}_3. \quad (10)$$

All the Nb/Al₂O₃ specimens with d Al₂O₃ = 5 Å showed anisotropic 3D superconductivity. All the specimens with d Al₂O₃ ≥ 30 Å showed 2D superconductivity. The effective mass ratio m_{\perp}/m_{\parallel} of 2D multilayers is infinite and $H_{c2\parallel}(T)$ is described by eq. (8). Quasi-2D superconductivity is observable for d Al₂O₃ = 10 Å and 20 Å. In Figs. 1(a)~1(c), $H_{c2\parallel}(T)$ and $\xi_{\perp}(T)$ are plotted as a function of temperature T for typical specimens which show the crossover. The perpendicular coherence length $\xi_{\perp}(T)$ was estimated from the H_{c2} data by the use of the following relation based on the GL approximation:

$$\xi_{\perp}(T) = \phi_0^{1/2} \left[2\pi \frac{dH_{c2\perp}}{dT} (T_c - T) \right]^{-1/2} \times (m_{\parallel}/m_{\perp})^{1/2}. \quad (11)$$

In the figures a horizontal line is drawn at $\xi_{\perp} = \lambda/1.4$ for each multilayer. According to DE, the cross point of the horizontal line and the $\xi_{\perp}(T)$ curve gives the crossover temperature T^* and $H_{c2\parallel}(T)$ should show an upturn near T^* . In Figs. 1(a)~1(c), we see that the upturn actually occurs slightly above the cross point. The prediction of Deutscher and Entin-Wohlman seems to be consistent with our experimental results.

The Nb/Al₂O₃ multilayers with d Al₂O₃ = 10 Å show 3D superconductivity for d Nb ≤ 50 Å and quasi-2D superconductivity for d Nb ≥ 60 Å. An example of $H_{c2\parallel}(T)$ and $\xi_{\perp}(T)$ of the 3D specimen with d Al₂O₃ = 10 Å is shown in Fig. 2. The $\xi_{\perp}(T)$ curve of the 3D multilayers does not cross the horizontal $\lambda/1.4$ line, which is also consistent with the DE prediction. The Nb/Al₂O₃ multilayers with d Al₂O₃ = 20 Å show 3D superconductivity for d Nb = 20 Å, quasi-2D superconductivity for 30 Å ≤ d Nb ≤ 40 Å and 2D superconductivity for d Nb ≥ 60 Å. For an example of the 2D multilayer with d Al₂O₃ = 20 Å $H_{c2}(T)$ of Nb(60 Å)/Al₂O₃(20 Å) is shown in Fig. 3. These results indicate that the effect of the

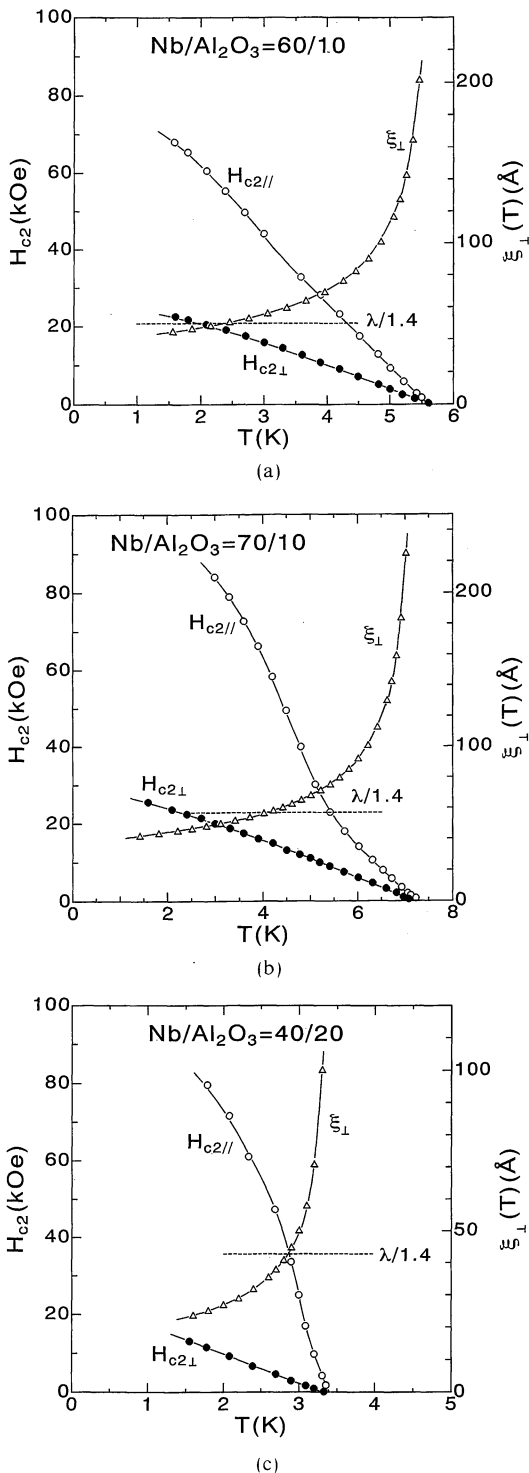


Fig. 1. $H_{c2\parallel}$ and $\xi_{\perp}(T)$ vs T for quasi-2D superconducting multilayers. (a) d Nb/ d Al₂O₃ = 60 Å/10 Å, (b) 70 Å/10 Å, (c) 40 Å/20 Å. $\xi(T)$ curves cross the horizontal dotted line drawn at $\lambda/1.4$ for each multilayer.

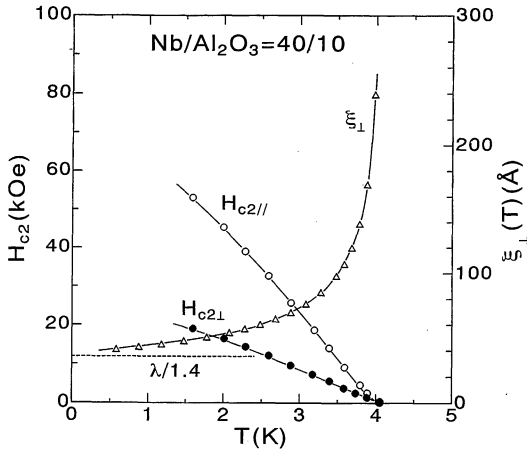


Fig. 2. An example of $H_{c2\parallel}(T)$ and $\xi_{\perp}(T)$ for 3D multilayers, 40 Å/10 Å. $\xi(T)$ curves do not cross horizontal $\lambda/1.4$ line.

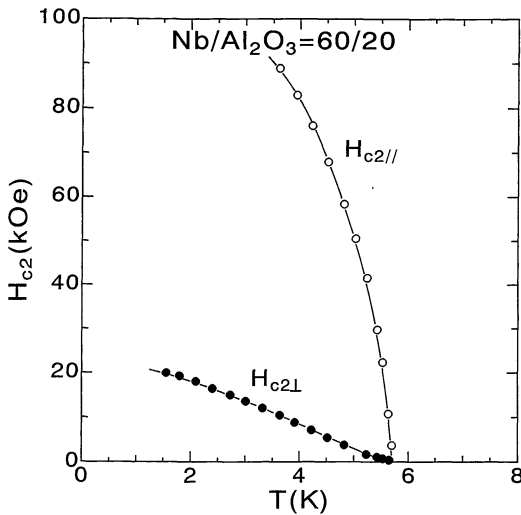


Fig. 3. An example of $H_{c2\parallel}(T)$ and $H_{c2\perp}(T)$ for 2D multilayers, 60 Å/20 Å.

Al₂O₃ layer thickness on the dimensionality of superconductivity is of essential importance as expected. But we must not overlook the fact that the effect of d Nb is also very significant. From the present results, it is evident that the larger d Nb values contribute to reduce the superconductive dimensionality. The origin which causes the d Nb dependence of the dimensionality may be qualitatively understood in the following way. Since the number of Cooper pairs in a single Nb layer is proportional to d Nb, the tunneling of a larger num-

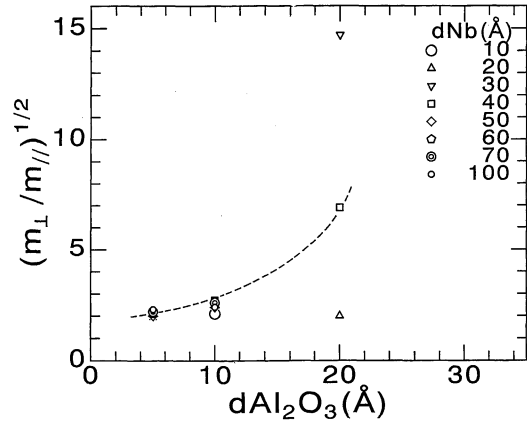


Fig. 4. The root of the mass ratio $(m_{\perp}/m_{\parallel})^{1/2}$ vs d Al₂O₃. The drastic enhancement of m_{\perp}/m_{\parallel} occurs between d Al₂O₃=10 Å and 20 Å. The guide line for eyes is drawn for d Nb=40 Å.

ber of Cooper pairs to the adjacent layer is necessary to result in sizable interlayer coupling between thicker Nb layers. Thus the Nb/Al₂O₃ multilayers with larger d Nb tend to show lower superconductive dimensionality for a fixed d Al₂O₃, i.e., for a fixed tunneling energy J .

In Fig. 4 we plot the square root of the mass ratio $(m_{\perp}/m_{\parallel})^{1/2}$ vs. d Al₂O₃ for 3D and quasi-2D multilayers. The ratio was determined from the temperature gradient of critical fields by the relation of eq. (3). As can be seen, the mass ratio sharply rises between d Al₂O₃=10 Å and 20 Å except for Nb(20 Å)/Al₂O₃(20 Å) which is a 3D superconductor. It should also be noticed that for d Al₂O₃=20 Å the superconductivity of multilayers with d Nb \geq 60 Å is 2D with $(m_{\perp}/m_{\parallel})^{1/2}$ values of infinity as is shown in Fig. 3. In the Nb/Ge system, the corresponding sharp of the ratio occurred in the vicinity of the Ge layer thickness d Ge \approx 30 Å. In the Josephson-coupling model, m_{\perp}/m_{\parallel} is inversely proportional to J^2 as is given by eq. (6). For a fixed barrier layer thickness, the tunneling energy J is smaller in the Nb/Al₂O₃ system than the Nb/Ge system. Al₂O₃ is an intrinsic insulator, while Ge is a semiconductor. The larger gap in the electron energy band of Al₂O₃ may contribute to make the Al₂O₃ sublayer the more efficient tunneling barrier than the Ge sublayer.

We calculated the parameter γ defined by

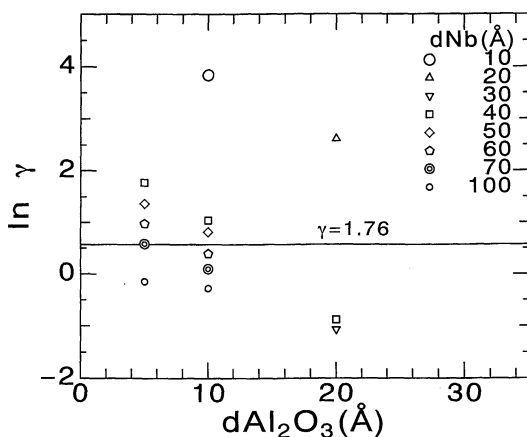


Fig. 5. $\log \gamma$ vs $d\text{Al}_2\text{O}_3$. The horizontal line shows $\gamma=1.76$, by which superconductive dimensionality is divided into 3D (above the line) and quasi-2D (below the line) according to the KLB theory. This criterion is satisfied by all multilayers except Nb(100 Å)/Al₂O₃(5 Å).

KLB using eq. (5) and $\log \gamma$ vs. $d\text{Al}_2\text{O}_3$ is plotted for $d\text{Al}_2\text{O}_3=5, 10$ and 20 Å in Fig. 5. We notice in the figure that all the sample with $\gamma > 1.76$ show 3D superconductivity and all the sample with $\gamma < 1.76$ show quasi-2D superconductivity in accord with the KLB theory. Only exception is Nb(100 Å)/Al₂O₃(5 Å) with 3D superconductivity, the γ value of which is 0.95. From measurements of general transport properties, we have earlier suggested that

$d\text{Al}_2\text{O}_3=5$ Å may be too small to form well-defined tunneling barriers in the Nb/Al₂O₃ system, though the existence of a layer-like modulated structure was verified by the satellite peaks of the small angle X-ray diffraction.¹⁹⁾ The discrepancy of the KLB γ value criterion for Nb(100 Å)/Al₂O₃(5 Å) may be attributable to the imperfect barrier formation.

Finally we summarize in Table I several superconducting material parameters of the Nb/Al₂O₃ multilayers discussed in this paper.

§4. Conclusion

1. The dimensional crossover has been studied for the Josephson coupled Nb/Al₂O₃ multilayers by varying the ratio of the superconducting Nb layer thickness $d\text{Nb}$ to the structural modulation wavelength λ . The crossover occurs, independent of $\lambda/d\text{Nb}$, in the vicinity of T^* where the perpendicular coherence length ξ_{\perp} is equal to $\lambda/1.4$. This result is in agreement with the calculation due to Deutscher and Entin-Wohlman.

2. We have experimentally confirmed that the crossover temperature T^* depends upon not only the tunneling barrier thickness ($d\text{Al}_2\text{O}_3$) but also the superconducting layer thickness ($d\text{Nb}$).

3. The effective mass ratio m_{\perp}/m_{\parallel} of the Nb/Al₂O₃ multilayer sharply increases between $d\text{Al}_2\text{O}_3=10$ Å and 20 Å. In the Nb/Ge

Table I. Superconducting parameters of Nb/Al₂O₃ multilayers.

$d\text{Nb}/d\text{Al}_2\text{O}_3$ (Å/Å)	T_c (K)	$dH_{c2\perp}/dT$ (kOe/K)	$dH_{c2\parallel}/dT$ (kOe/K)	$(m_{\perp}/m_{\parallel})^{1/2}$	$\xi_{\perp}(0)$ (Å)	γ	$\ln \gamma$	$\xi_{\parallel}(0)$ (Å)	Dimension
40/5	3.496	9.9	20.0	2.0	48.2	5.85	1.17	97.5	3D
50/5	4.395	8.0	16.1	2.0	48.0	3.88	1.36	96.7	3D
60/5	4.825	7.4	15.2	2.1	46.7	2.63	0.97	96.0	3D
70/5	5.539	6.2	13.7	2.2	44.3	1.78	0.58	97.9	3D
100/5	6.599	5.2	11.8	2.3	43.1	0.86	-0.15	97.9	3D
10/10	1.810	11.8	24.2	2.1	60.5	46.6	3.84	124.1	3D
40/10	4.080	8.0	21.5	2.7	37.3	2.83	1.04	100.4	3D
50/10	5.000	7.2	17.3	2.4	39.8	2.24	0.81	95.6	3D
60/10	5.661	6.3	16.0	2.5	37.8	1.48	0.39	96.1	q-2D
70/10	7.217	4.8	12.5	2.6	37.4	1.11	0.10	97.5	q-2D
100/10	6.979	4.6	11.0	2.4	42.3	0.75	-0.28	101.2	q-2D
20/20	1.873	9.7	19.8	2.0	65.9	13.8	2.62	134.6	3D
30/20	3.013	3.0	44.0	14.7	13.0	0.34	-1.07	120.0	q-2D
40/20	3.398	7.0	48.0	6.9	17.1	0.41	-0.88	120.0	q-2D

system due to Ruggiero *et al.*,¹⁾ the corresponding increase of m_{\perp}/m_{\parallel} was observed at about $d_{\text{Ge}} \approx 30 \text{ \AA}$. This results indicate that the Al₂O₃ insulator layer forms more efficient tunneling barrier in Nb based superlattice than the Ge semiconductor layer.

Acknowledgements

Authors wish to thank Dr. Y. Kamiguchi for his experimental contribution and valuable discussion.

References

- 1) S. T. Ruggiero, T. W. Barbee, Jr. and M. R. Beasley: Phys. Rev. **B26** (1982) 4894.
- 2) C. S. L. Chun, G. G. Zheng, J. L. Vincent and I. K. Schuller: Phys. Rev. **B29** (1984) 4915.
- 3) I. Banerjee and I. K. Schuller: J. Low Temp. Phys. **54** (1984) 501.
- 4) J. L. Cohn, J. J. Lin, F. J. Lamelas, H. He, R. Clarke and C. Uher: Phys. Rev. **B38** (1988) 2326.
- 5) D. Neerincx, K. Temst, C. V. Haesendonck, Y. Bruynseraede, A. Gilabert and I. K. Schuller: Phys. Rev. **B43** (1991) 8676.
- 6) V. L. Ginzburg and L. D. Landau: Zh. Eksp. Teor. Fiz. **20** (1950) 1064.
- 7) K. Maki: Phys. Rev. **148** (1966) 362.
- 8) See, for example, D. E. Proker, R. E. Schwall and M. R. Beasley: Phys. Rev. **B21** (1980) 2717; M. Ikebe and Y. Muto: Synthetic Metals **5** (1983) 229.
- 9) Y. Obi, M. Ikebe, Y. Fukumoto, Y. Muto and H. Fujimori: *JJAP Ser. I Superconducting Materials*, ed. S. Nakajima and H. Fukuyama (Jpn. J. Appl. Phys., Tokyo, 1988) p. 129.
- 10) K. Kanoda, H. Mazaki, T. Yamada, N. Hosoi and T. Shinjo: Phys. Rev. **B33** (1986) 2052.
- 11) P. G. de Gennes and E. Guyon: Phys. Lett. **3** (1963) 168.
- 12) N. R. Werthamer: Phys. Rev. **132** (1963) 2440.
- 13) P. G. de Gennes: Rev. Mod. Phys. **36** (1964) 225.
- 14) S. Takahashi and M. Tachiki: Phys. Rev. **B33** (1986) 4620.
- 15) W. E. Lawrence and S. Doniach: *Proc. 12th Int. Conf. Low Temperature Physics, 1970*, ed. E. Kanda (Academic Press of Japan, Tokyo, 1971) p. 361.
- 16) R. A. Klemm, A. Luther and M. R. Beasley: Phys. Rev. **B12** (1975) 877.
- 17) M. Tachiki and S. Takahashi: Physica **135B** (1985) 178.
- 18) M. Tachiki and S. Takahashi: Physica **C153-155** (1988) 1702.
- 19) Y. Kamiguchi, M. Ikebe, Y. Obi and H. Fujimori: Jpn. J. Appl. Phys. **30** (1991) 945.
- 20) Y. Kamiguchi, Y. Obi, M. Ikebe and H. Fujimori: *Proc. the MRS Int. Meet. Advanced Materials, 1988*, ed. M. Doyama, S. Somiya and R. P. H. Chang (Materials Research Society, Pittsburgh, Pennsylvania, 1989) Vol. 10, p. 3.
- 21) G. Deutscher and O. Entin-Wohlman: Phys. Rev. **B17** (1978) 1249.